16,10,08

Comparative analysis of optical properties $C-Gd_2O_3:Eu^{3+}$ single crystal and nanocrystalline sample

© V.V. Bakovets, M.S. Tarasenko, R.E. Nikolaev, T.D. Pivovarova, I.V. Yushina, A.A. Ryadun, I.P. Dolgovesova, N.G. Naumov

Federal State Budgetary Institution of Science Institute of Inorganic Chemistry after A.V. Nikolaev Siberian branch of Russian Academy of Science, Novosibirsk, Russia

E-mail: becambe@niic.nsc.ru

Received June 21, 2024
Revised July 19, 2024
Accepted July 28, 2024

Single crystals (SC) of $C-Gd_2O_3$ were grown from a solution in a $Li_6Gd(BO_3)_3 + Gd_2O_3 + Eu_2O_3$-flux with seed using Czochralski method. Growing was carried out at a relatively low temperature of 1145°C. A sample of nanocrystallites powder (NCP) was obtained by the sol-gel method from aqueous solutions of $Gd(NO_3)_3$ and $Eu(NO_3)_3$ with NaOH-precipitant by dispersed spraying of these solutions. The obtained SC and NCP C $C-Gd_2O_3:Eu^{3+}$ samples were analyzed by X-ray powder diffraction (XRD) to confirm the $C-Gd_2O_3$ cubic phase formation and to determine both the sizes (59 nm) and the deformation stresses (0.06%) of nanoparticles. It has been shown, when the photoluminescence (PL) excitation energy changes over the series 250, 280, and 300 nm, then low-energy PL bands at 620 and 710 nm decrease in intensity relative to the intensity of main PL band at 611 nm. For high-energy bands at 595, 550, 480, 470 and 420 nm, an increase in their intensity relative to the 611 nm band is observed. High-energy bands are not visible against the background noise for NCP. A study of diffuse reflection (DR) spectra showed the charge transfers along PL radiative transitions are not direct and are carried out with the participation of phonons at energy of 0.29 eV for the bulk part of the SC and 0.26 eV for the damaged surface layer of the SC formed during mechanical polishing. Higher phonon energy of 0.49 eV is observed for NCPs, this is due to the large surface area of the particles and that correlates with the broadening of the XRD reflections at half maximum.

Keywords: cubic gadolinium oxide, single crystal and nanocrystallite sample, photoluminescence activator Eu^{3+} ions, diffusion reflection, photoluminescence energy redistribution.

DOI: 10.61011/PSS.2024.09.59231.160

1. Introduction

Oxides of rare earth elements (REE), doped with Eu^{3+} ions are effective phosphors of red region of radiation [1–3]. Y_2O_3 and Gd_2O_3 oxides are the most acceptable for these purposes in current engineering, in view of acceptability and price, at that intensity of photoluminescence (PL) of $Gd_2O_3:Eu^{3+}$ is significantly higher. In current engineering powder-like phosphors are used, e.g. $Gd_2O_3:Eu^{3+}$ of different degree of dispersion. Definite dispersion provision may in somewhat improve the phosphor efficiency. We understand that this approach results in change in specific area of powder sample crystallites. As a result the surface composition of crystallites has increased activity to adsorption of both matrix material elements, and of environment admixtures. This, in turn, affects the color and brightness characteristics of phosphor. Scientifically justified understanding of nature of PL processes is complicated by the fact that in the cubic modification of the matrix $C-Gd_2O_3$ sp.gr. Ia-3 (JCPDS 86-2477) the cations are distributed in two different positions in cation sublattice: centrosymmetric inversion $C_{3i}(S_6)$ and noncentrosymmetric C_2 [4,5]. It was noted that in this lattice the theoretical ratio of cations in positions C_2 ($24d$) and C_{3i} ($8b$) is 3. At that cations in position C_2, being in noncentrosymmetric environment, are very sensitive to distortion of the environment of crystal field, and cations in position C_{3i} in ideal lattice are not sensitive to distortion of the environment crystal field. As a result spectra of their PL can somewhat change by wavelength of top of radiation bands, and can significantly change by intensity. It is difficult to differentiate positions C_2 of cations from cations located on defect surface of crystallites. In this sense, in a single-crystal sample the identification of PL bands in its volume will be freed from the influence of surface phenomena. Large single-crystals Gd_2O_3 can be used as optical elements in modern physics of elementary particles, and also in planar technology of optical and electronic integral devices as base substrates. This is associated with unique dielectric and optical parameters of this material. Unfortunately, use of Czochralski method and others to grow large crystals from melt, for Gd_2O_3 is impossible due to their high melting point ~ 2340°C and presence of phase transformations [6].

Recently relatively large (1–2 cm) single-crystals of $Ln_2O_3:Ln^{3+}$ with high transparency in optical range were obtained by Czochralski method from solution-

melt [7–9,10,11] at relatively low temperature in range 1200−1300°C. But single-crystals $C-Gd_2O_3:Eu^{3+}$ were not grown due to absence of solvent optimal state. Optimization of composition of melt solution $Li_6Gd(BO_3)_3-Gd_2O_3$, doped with Eu^{3+} ions [1,12], ensured growth of single-crystals with size up to 2 cm. The present paper task is the comparative analysis of PL optical spectrum and diffusion reflection of single-crystals and nanodisperse powder samples of effective phosphor $C-Gd_2O_3:Eu^{3+}$.

2. Experimental part

Single-crystals $C-Gd_2O_3$, doped with Eu^{3+}, were grown using the single-crystal Czochralski low-gradient method from melt $Li_6Gd(BO_3)_3$, as described in detail in papers [1,7,8,12]. During synthesis we take in stoichiometric ratio Li_2CO_3, H_3BO_3 and Gd_2O_3 in amount required to obtain 300 g $Li_6Gd(BO_3)_3$. The solvent was synthesized in platinum crucible in two stages. At first stage the crucible with precursors was loaded in muffle furnace and heated in air with rate 5 deg/h to temperature 400°C. After holding at 400°C for 24 h the furnace was gradually cooled to room temperature. At second stage of synthesis the crucible was reloaded in the furnace with inert atmosphere (Ar $\geq$ 99.98%) and heated to 1000°C with rate 40 deg/h. crucible with melt was held at 1000°C for 24 h, and then cooled to room temperature. Powders Gd_2O_3 and Eu_2O_3 were loaded into crucible with $Li_6Gd(BO_3)_3$ in amount required to obtain 20 mol% of oxides excess relative to borate-solvent, and to obtain total ratio Gd:Eu in melt equal to 99:1. Preliminary prepared crucible with melt solvent was loaded into the chamber with argon to grow crystal, and heated to 1145°C with rate 60 deg/h. To ensure homogenization the melt was held at 1145°C for 72 h. Single-crystal $C-Gd_2O_3:Eu^{3+}$ was grown at temperature 1145°C on seed (small crystal $C-Gd_2O_3$), oriented perpendicular to natural facet (211). Polished wafers cut from theses crystals are 1 mm thick [12]. Actual concentration of europium ions 1.1 mol% in grown single-crystal was determined by chemical analysis method. According to data of element analysis amount of Li and B comprising the solvent $Li_6Gd(BO_3)_3$ in grown crystals does not exceed 10^{-5} wt%. As per diffractometry data the grown crystal $C-Gd_2O_3:Eu^{3+}$ has cubic structure of bixbyite.

To obtain nanostructured phosphors based on $C-Gd_2O_3$, doped with ions Eu^{3+}, the sol-gel method was used [13]. $Gd(NO_3)_3\cdot 6H_2O$ and $Eu(NO_3)_3\cdot 5H_2O$ nitrides obtained from appropriate oxides with basic components content at least 99.9% were used in paper as reagents. Concentration of $Eu(NO_3)_3\cdot 5H_2O$ was selected based on Eu^{3+} content 3.5 mol% in solid solution of oxides. To obtain precursors of hydroxides we used 0.2M solutions of nitrates corresponding to above said percentage ratio of oxides content. A twofold molar excess of NaOH solution of „extra pure“ grade in double-distilled water was used as a precipitator. Methodic details of synthesis are presented earlier in paper [13] and previous papers of authors.

The obtained sediment of hydroxides was washed out to neutral value pH of washing fluids, dried in air in thermostatic chamber and then annealed in the muffle furnace at 1200°C. Chemical analysis of product composition showed ratio of atoms Eu/Gd = 4.5 mol%. Increased content of Eu^{3+}, relative to initial amount (3.5 mol%) in sol-gel process is, probably, associated with lower rate of hydrolysis of $Gd(NO_3)_3$ and insufficiency of time of product complete ageing in solution. The obtained nanocrystalline samples $C-Gd_2O_3:Eu^{3+}$ have cubic structure of bixbyite.

X-ray diffraction analysis of structure and size of crystallites was carried out using Shimadzu XRD-7000 (CuK_αemission, Ni-filter diffractometer, range 5−70° 2θ, interval 0.03°, uptake 2 s).

Luminescence spectra were studied using Cary Eclipse (VARIAN) fluorescent spectrophotometer, excitation wavelength 250, 280 and 300 nm. Minimum step of detector 0.1 nm. Spectral resolution 0.1 nm. PL excitation spectra were not specified.

Diffuse reflectance (DR) spectra $R_d = f(\lambda)$ of powders were recorded by a standard method using UV-3101PC (Shimadzu) spectrophotometer in the wavelength range λ from 240 to 800 nm. UV and visible range wavelength axis calibration accuracy was ± 0.3 nm, wavelength reproducibility was ± 0.1 nm. Measurement errors due to light scattering were 0.01%. $BaSO_4$ was used as a standard. The powder DR spectra were used to calculate the samples' optical absorption in relative units using the classical Kubelka−Munk function (K−M) [14] and the band gap E_g was found using a Tauc plot as per the following equation [15]

$$[F(R_d)h\nu] = [(1-R_d)^2/(2R_d)h\nu] = C(h\nu - E_g)^n, \quad (1)$$

where R_d — the value of sample's optical reflection in relation to the reference reflection, h — the Planck's constant, ν — reflected light wave frequency, C — constant, n — index of power.

3. Experimental results and discussion

Figure 1 shows diffraction patterns of samples of nanocrystalline powder and single-crystal.

The diffraction patterns correspond to the cubic modification $C-Gd_2O_3$ sp.gr. (Ia-3) (PDF № 86-2477). Parameter of elementary lattice of nanopowder obtained by sol-gel method, $a = 10.826$ Å (standard deviation $S_a = 0.01$) and for micron powder sample obtained by grinding the single-crystal $a = 10.8106$ Å [12], this corresponds to phase $C-Gd_2O_3$ (JCPDS card 12−0797). The insert shows the comparison of intensities of plain (222) reflex of both samples. No monoclinic phase was detected, as the metastable cubic phase is stabilized by the presence of Eu^{3+} ions [16,17]. The horizontal strips at half-height level of each reflex clearly show large width for nanocrystalline sample. Calculation of values of coherent

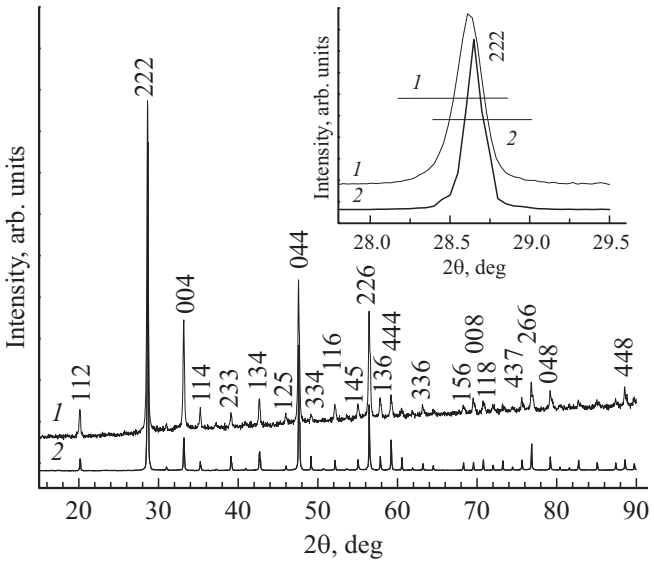

Figure 1. The diffraction pattern of samples of nanocrystalline powder $C-Gd_2O_3:Eu^{3+}$ (4.5 mol%) — *1* and single-crystal ground to particles of micrometer size $Gd_2O_3:Eu^{3+}$ (1 mol%) — *2*. In insert sections *1* and *2* designate half-height of reflexes (222).

scattering region as per Hall–Williamson method [18] gives the averaged value of size of nanoparticles 59 ± 5 nm and the diffraction component 0.06%. These facts mean that for the nanocrystalline sample the specific area is much higher then for the microcryctalline sample obtained by single-crystal grinding, and, accordingly, contains large number of deformed lattice corners, in particular also on surface of particles.

Figure 2 presents PL spectra of single-crystals and nanopowders $C-Gd_2O_3:Eu^{3+}$.

Spectra of luminescence at excitation energies 250 and 280 nm (4.96 and 4.43 eV respectively) practically do not change. In case of excitation in line 300 nm (4.13 eV) for single-crystal the intensity of bands 420 nm of transition $^5D_3 \rightarrow {}^7F_j$ and 470 nm of transition $^5D_2 \rightarrow {}^7F_0$ significantly increase (see insert in Figure 2, *g*). Intensity of bands 480 nm of transition $^5D_2 \rightarrow {}^7F_j$ and 550 nm — $^5D_1 \rightarrow {}^7F_j$ significantly increases relative to intensity of band 611 nm of transition $^5D_0 \rightarrow {}^7F_2$. It is obvious that for PL excitation line 300 nm energy of radiation transition $^5D_0 \rightarrow {}^7F_2$, band 611 nm decreases (Figure 2, *a, b*). For nanocrystalline sample the high-energy bands are not observed, probably,

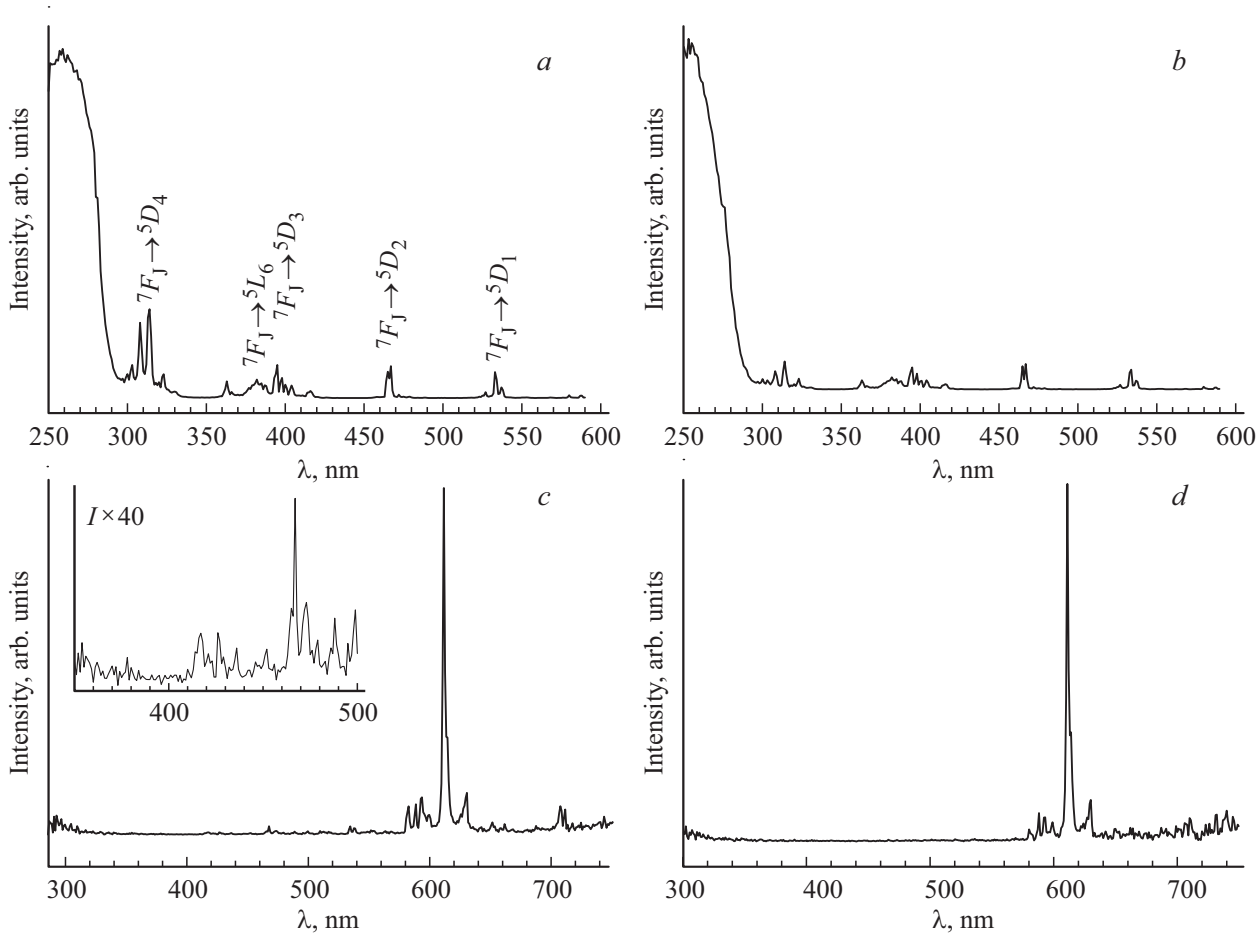

Figure 2. Excitation spectra (*a, b*) (for PL band 611 nm) and PL spectra (*c–g*) for spectral excitation lines 250, 280 and 300 nm ((*c, d*), (*e, f*) and (*g, h*) respectively) for single-crystal (*a, c, e, g*) nanostructured sample (*b, d, f, h*). The inserts present PL spectra in region of small wavelengths.

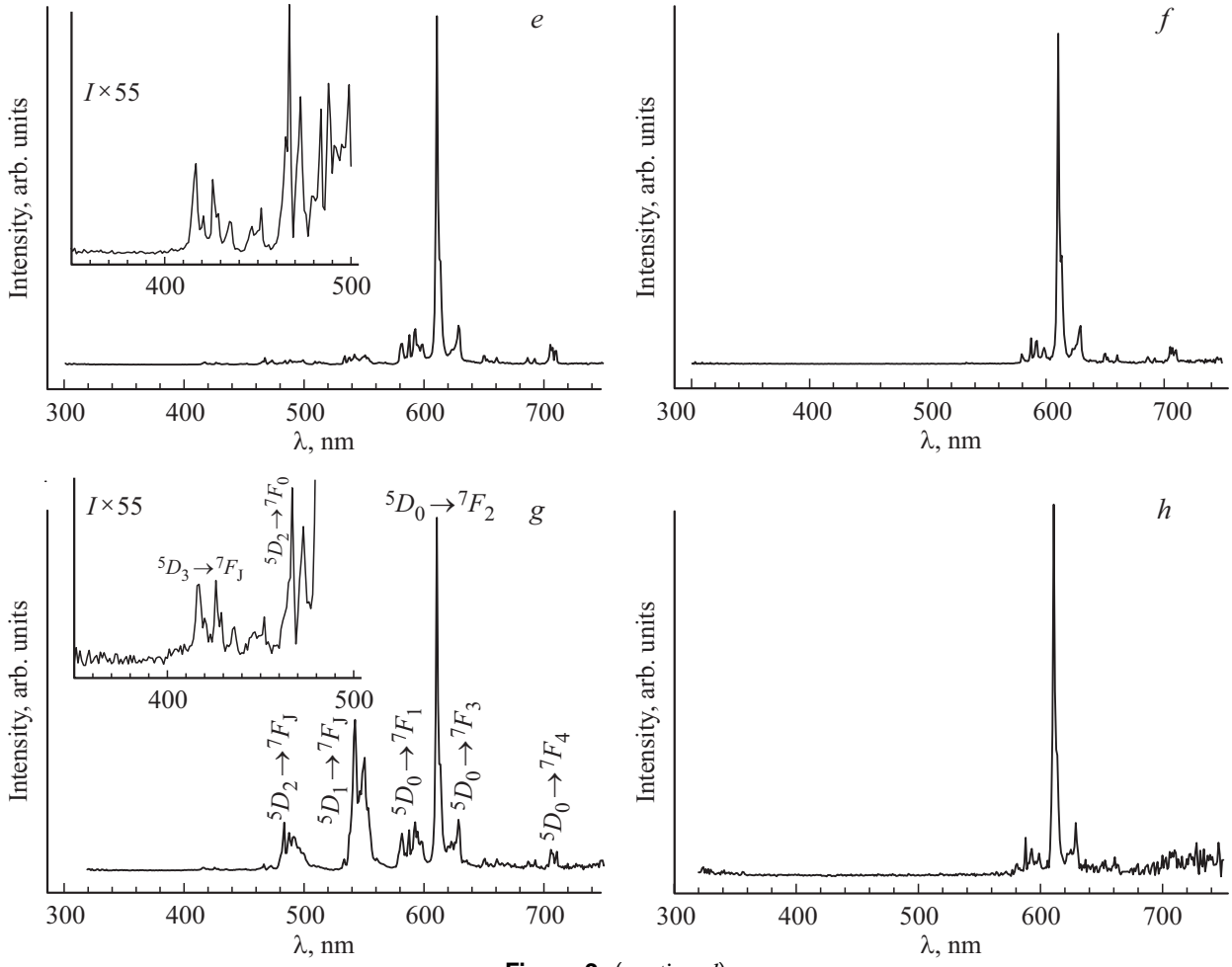

Figure 2 (*continued*).

due to string scattering of excitation energy on surface of nanocrystals. It is specifically that brightness of illumination of nanocrystalline sample is significantly lower PL brightness of single-crystal, for which excitation energy scattering is observed on boundaries of the nanocrystallites. This is especially clearly observed in the high-energy region 300−400 nm of PL spectrum (Figure 2, *f, h*).

The nature of the redistribution of the PL excitation energies along the radiative transitions can be analyzed by the change in the ratio of PL bands with the base intensive band 611 nm when the excitation energy changes along the series of 250, 280 and 300 nm lines.

Figure 3 presents calculations of values I_{611}/I_λ of ratio of intensities of PL bands to intensity of base band 611 nm.

For single-crystal sample in center and at edge of crystal the ratios of intensities of bands I_{611}/I_{593} and I_{611}/I_{630} practically stay equal at excitation energies 250 and 280 nm. This indicates a good reproducibility of the electronic structure and, consequently, a good uniformity of the single-crystal through its volume. When excitation energy decreases to 300 nm the ratios I_{611}/I_{470} and I_{611}/I_{550} decrease by value of more methodical error 5% (Figure 3, *c*) and Symbatly with significant decrease in intensity of band I_{611} (see Figure 2, *a*). When transferring to next radiation band 710 nm we observe increase in ratios I_{611}/I_{710} for all excitation energies 250, 280 and 300 nm, at that in a greater extent for excitation energies 250 and 300 nm. At excitation energies 280, and especially 300 nm, the radiation intensity of band 611 nm approach very low values (Figure 2, *a, b*).

For the nanocrystalline sample the nature of the change in the intensity ratios of the PL bands in the region 611−710 nm is practically same as changes for single-crystals. But ratio of intensities of bands 611 and 620 nm significantly decreases, this means intensity increasing of band 620 nm. Bands of region of radiation high energies are mot observed at background of noises (inserts *b, d, f, h* Figure 2), this, probably, is associated with the influence of the defectiveness of a large set of interfaces of nanocrystalline powder on the PL spectra.

The characteristic feature of ratios change of PL bands intensity to band 611 nm intensity for single-crystal is ratios increasing for the region of low-energy bands of radiation 620 and 710 nm, and ratios decreasing of bands in region of high energies 420, 470, 480 and 550 nm at relatively low excitation energy 300 nm. At that, intensities of these

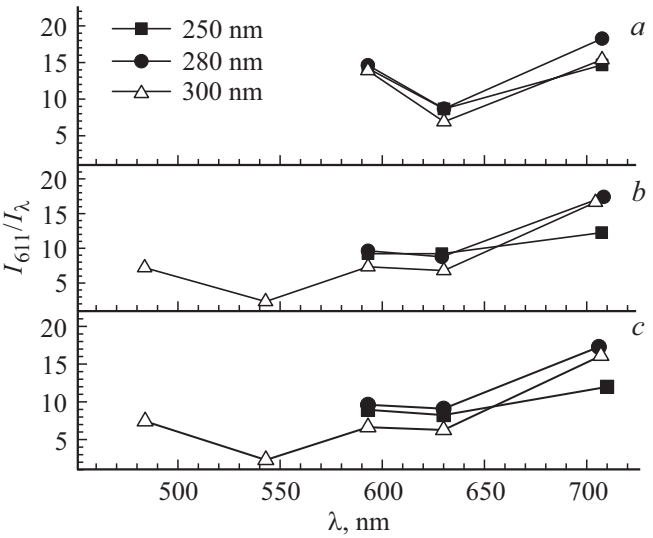

Figure 3. Change in ratios of intensities of PL bands to band 611 nm for nanocrystalline sample (*a*), center of single-crystal (*b*) and edge of single-crystal (*c*) at said excitation energies.

radiation bands clearly increase. This is possible only with the phonons participation in the charge transfer.

When studying the diffraction patterns of the samples, the large defectiveness of the nanocrystalline sample was determined (Figure 1, insert). It is known that increase in the defectiveness of crystalline structures is accompanied by complication of the phonon spectrum, and increase in the total energy of the phonons that make it up.

We think that study of DR spectrum from surface of the single-crystal and powder nanocrystalline sample can determine the phonons participation in charges transfer. Figure 4 presents DR spectra of single-crystal (Figure 4, *a, b*) and nanocrystalline sample (Figure 4, *c*), obtained as per Kubelka–Munk model [14] in Tauc coordinates [15].

We see that DR curve of single-crystal is presented by two regions (Figure 4, *a, b*), their mathematical processing ensures understanding that these regions characterize to reflection mechanisms. In high-energy region (above 4 eV) the curve is approximated by two straight lines at power exponent of parameter $(\mathrm{Abs}\cdot h\nu)^{1/2}$. This shows that charges transition is indirect, i.e. with phonons participation. Continuation of these straight lines to crossing with axis of abscisses gives the representation on width of gap of charges transfer to fundamental absorption edge of single-crystal sample. As the regression coefficient of such approximation is maximum, $R^2 = 0.9793$ for straight lime *1* and 0.9828 for straight line *2*, then gap width is $(Eg_1 + Eg_2)/2 = (4.26 + 3.68)/2 = 3.97$ eV and phonons energy is ± 0.29 eV. The corresponding calculations and construction for the low-energy region (less than 4 eV) are also approximated by two straight lines with an power of exponent 1/2 for the right-hand side of the equation *1*, which indicates the indirect transition of charges through the gap with parameters $Eg_1 = 3.85$ eV for straight line *1* and $Eg_2 = 3.33$ eV for straight line *2*. Then the gap width is $Eg_0 = 3.59$ eV, and phonons energy is 0.26 eV.

The obtained values of gap Eg_0 state that for the single-crystal sample there are two regions of diffuse reflectance spectrum. Region of high energies > 4 eV is, probably, associated with bulk portion of crystal, as parameter $Eg_0 = 3.97$ eV maximum for single-crystal $C-Gd_2O_3:Eu^{3+}$ (1 mol%) at known band gap 5.6 eV for single-crystal $C-Gd_2O_3$. Region of low energies < 4 eV is associated

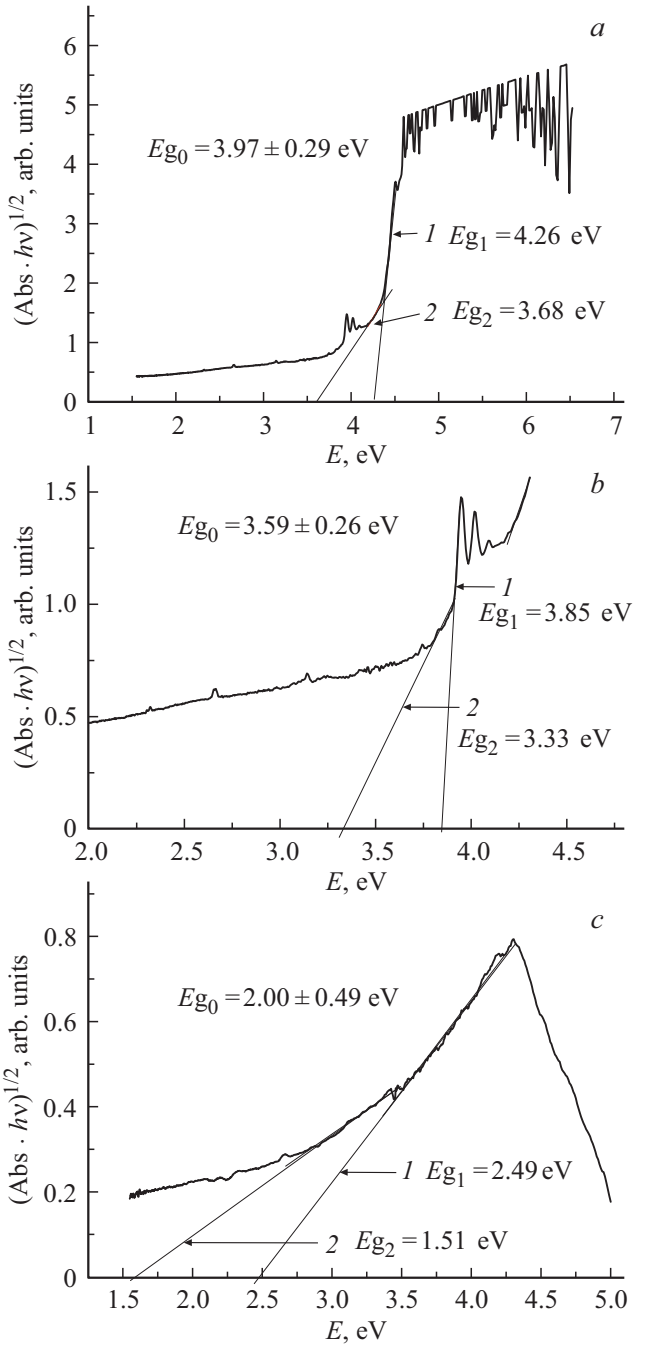

Figure 4. Diffuse reflectance spectra of single-crystal (*a, b*) and nanocrystalline sample (*c*).

with processes of reflection from destructed layer of surface of single-crystal, for which parameter is $Eg_0 = 3.59$ eV. This is natural, as the single-crystal passes through mechanical polishing at final stage of treatment by the grinding material $1\,\mu$m. Depth of this layer can reach $5-7\,\mu$m and over [19]. This damaged layer upon absence of chemical polishing contains cluster of dislocations, package defects, cluster of vacancies, point defects and other disturbances of crystal lattice. These disturbances are traps of charges and can create non-degenerate regions of cations at bottom of conduction band, or of anions at top of valence band. This results in decrease of gap of charges transition from basic state to series of orbitals $^7F_0 \rightarrow {}^5D_j$ of cations Eu^{3+} at low PL excitation energies 300 nm. At that for single-crystal participation of phonons causes radiation of increased energies via transitions $^5D_j \rightarrow {}^7F_j$ (Figure 2, *g*).

So, we can make the known conclusion that at average excitation energies 250−280 nm the energy is transferred by transfer of charges $Gd^{3+} \rightarrow O^{2-}$, $O^{2-}(2p) \rightarrow Eu^{3+}(4f)$ [20] and further via transition $Gd^{3+} \rightarrow Eu^{3+}$ to levels ^5D_j with further radiative transitions $^5D_j \rightarrow {}^7F_j$ [21,22] with participation of phonons. This, in turn, leads to radiation energy redistribution via PL bands, and this correlates with obtained results (Figure 4) on change of intensity of bands relative to base band of radiation 611 nm (Figure 3). Transitions of charges in both regions are indirect, and, therefore, with participation of phonons. The characteristic difference between phonons energy for considered samples: 0.26 eV for single-crystal and 0.49 eV for nanocrystalline sample. This, naturally, is associated with larger defectiveness of nanocrystals due to large specific area of nanocrystals of powder sample.

Note that some papers [12,21] provide the defectiveness analysis of matrix structure of compounds Gd_2O_3, $Gd_2O_3:Eu$, Tb and its effect on nature of charges transfer, and, therefore, on distribution of excitation and radiation energies of PL. We assume that for completeness and objectivity of information on nature of formation of the radiation spectra we need study results of actual structure of crystalline substances and nature of their phonon spectrum.

4. Conclusion

So, it is determined that PL spectra of single-crystals and nanocrystalline samples of cubic $C-Gd_2O_3:Eu^{3+}$ have definite set of differences. Mainly these differences of surface of single-crystal and interfaces of crystallites of nanocrystalline samples, in particular, by degree of their imperfection. The studied samples of single-crystals are characterized by presence of disturbed surface layer, which occurs during sample planes polishing without further polishing etching, which is necessary to delete the imperfections of the crystalline structure. The nanocrystalline sample is characterized by large specific area of interfaces, which due to their nature contain defects of lattice and strains. It is determined that in all cases the luminescence spectrum is formed not by direct charges transfer, but with participation of phonons. The phonons energy is determined by the deformation stresses and another defects of structure in bulk section of single-crystal, and, mainly, by deformed state of large specific area of nanocrystalline samples. This results in changes in energy distribution via the radiative transitions upon change of PL excitation energy. When excitation energy increases in range 250−300 nm the radiation energy distribution of bands 620 and 710 nm shifts towards decrease in their intensities relative to the intensity of band 611 nm. At that intensity of the band 611 nm significantly decreases. At the excitation energies 300 nm the intensity of base band of spectrum 611 nm is the lowest for the considered range of excitation energies, but at that the intensity of high-energy bands 420, 470, 480 and 550 nm increases relative to the intensity of band 611 nm. The obtained DR results state that these defects are associated with phonons energy determined by features of the actual structure of single-crystal bulk and its surface similarly as for nanocrystalline samples. Understanding of nature of relationships between the defectiveness of interfaces with features of energy distribution by PL radiation bands requires detail theoretical study, this is beyond the present experimental study.

Acknowledgments

The authors express their gratitude to I.V. Korol'kov for the X-ray diffraction analysis of nanocrystalline samples, A.V. Sotnikov for processing the diffraction patterns according to Hall−Williamson model.

Funding

The study was supported by the Ministry of Science and Higher Education of the Russian Federation, project No. 121031700315-2, Russian Scientific Foundation (project No. 22-43-02079).

Conflict of interest

The authors declare that they have no conflict of interest.

References

[1] V.A. Pustovarov, I.N. Ogorodnikov, R.E. Nikolaev, M.S. Tarasenko, D.A. Tavrunov, V.A. Trifonov, N.G. Naumov. Opt. Mater. **143**, 114265 (2023). https://doi.org/10.1016/j.optmat.2023.114265

[2] V.V. Bakovets, T.D. Pivovarova, P.E. Plyusnin, I.P. Dolgovesova, M.I. Rakhmanova, A.V. Sotnikov. Rus. J. Gen. Chem., **94**, *1*, 138 (2024). https://doi.org/10.1134/S1070363224010134

[3] R.E. Nikolaev, A.M. Yakovleva, M.S. Tarasenko, A.S. Sukhikh, V.A. Trifonov, N.G. Naumov. Zhurn. Strukt. Khim., **64**, *7*, 112774 (2023). (in Russian). https://doi.org/10.1134/S0022476623070041

[4] B. Antic, M. Mitric, D. Rodic, Y. Zhong, Y. Artemov, S. Bogdanovich, J.R. Friedman. Phys. Rev. B, **58**, *6*, 3212 (1998). https://doi.org/10.1103/PhysRevB.58.3212
[5] M. Mitric, P. Onnerud, D. Rodic, R. Tellgren, A. Szytula, M.L. Napijalo. J. Phys. Chem. Solids, 54, 8, 967 (1993). https://doi.org/10.1016/0022-3697(93)90226-H
[6] G.-Y. Adachi, N. Imanaka. Chem. Rev., **98** (1998). https://doi.org/10.1021/cr940055h
[7] P. Veber, M. Velázquez, V. Jubera, S. Péchev, O. Viraphong. CrystEngComm, **13**, *16*, 5220 (2011). https://doi.org/10.1039/c1ce00015b
[8] P. Veber, M. Velázquez, G. Gadret, D. Rytz, M. Peltz, R. Decourt. CrystEngComm, **17**, *3*, 492 (2015). https://doi.org/10.1039/c4ce02006e
[9] F. Druon, M. Velázquez, P. Veber, S. Janicot, O. Viraphong, G. Buşe, M.A. Ahmed, T. Graf, D. Rytz, P. Georges. Opt. Lett., **38**, *20*, 4146 (2013). https://doi.org/10.1364/OL.38.004146
[10] A.A. Pavlyuk, Y.V. Vasiliev, L.Y. Kharchenko, F.A. Kuznetsov, Low thermal gradient technique and method for large oxide crystals growth from melt and flux, Proc. Of APSAM-92 (Asia Pacific Society for Advanced Materials.), Shanghai, China, 1993, pp. 164.
[11] Ya.V. Vasil'ev, I.A. Borovlev, E.N. Galashov, N.V. Ivannikova, F.A. Kuznetsov, A.A. Pavlyuk, I.G. Stenin, V.N. Schlegel. Nizkogradientnaya tekhnologiya rosta stsintillyatsionnykh oksidnykh kristallov. ISMA, Khar'kov, 2011. (in Russian).
[12] V.A. Pustovarov, R.E. Nikolaev, V.A. Trifonov, M.S. Tarasenko, S.J. Dhoble, D.A. Tavrunov, N.G. Naumov. Opt. Mater., **141**, 113966 (2023). https://doi.org/10.1016/j.optmat.2023.113966
[13] V.V. Bakovets, L.N. Trushnikova, I.V. Korol'kov, P.E. Plyusnin, I.P. Dolgovesova, T.D. Pivovarova, N.I. Alferova. Russian Journal of General Chemistry, **83**, 3 (2013). https://doi.org/10.1134/S1070363213010015
[14] P. Kubelka, F. Munk. Z. Techn. Phys., **12**, 593 (1931).
[15] J. Tauc, R. Grigorovici, A. Vancu. Phys. Status Solidi B, **15**, *2*, 627 (1966). https://doi.org/10.1002/pssb.19660150224
[16] P.P. Fedorov, M.V. Nazarkin, R.M. Zakalyukin. Crystall. Rep., **47**, *2*, 316 (2002). https://doi.org/10.1134/1.1466504
[17] R. Srinivasan, N.R. Yogamalar, J. Elanchezhiyan, R.J. Joseyphus, A.C. Bose. Journal of Alloys and Compounds, **496**, *1*, 472 (2010). https://doi.org/10.1016/j.jallcom.2010.02.083
[18] S.S. Pushkarev, M.M. Grekhov, N.V. Zenchenko. FTP, **52**, *6*, 586 (2018). (in Russian). https://doi.org/10.21883/FTP.2018.06.45920.8661
[19] S.N. Nikiforova-Denisova. Tekhnologiya poluprovodnikovykh priborov i izdelij mikroelektroniki. Vysshaya shkola, M., 1989. (in Russian).
[20] Z. Wang, P. Wang, J. Zhong, H. Liang, J. Wang. J. Lumin., **152**, 172 (2014). https://doi.org/10.1016/j.jlumin.2013.11.040
[21] Y.A. Kuznetsova, A.F. Zatsepin, R.A. Tselybeev, V.N. Rychkov, V.A. Pustovarov. J. Phys. Conf. Ser., **741**, *1*, 012089 (2016). https://doi.org/10.1088/1742-6596/741/1/012089
[22] V.V. Bakovets, S.V. Belaya, T.D. Pivovarova, I.P. Dolgovesova, I.V. Korolkov, O.V. Antonova, M.I. Rakhmanova. J. Lumin., **215**, 116633 (2019). https://doi.org/10.1016/j.jlumin.2019.116633

Translated by I.Mazurov